2024 IEEE/RSJ International Conference on Intelligent Robots and Systems (IROS)
October 14-18, 2024. Abu Dhabi, UAE

A non-invasive device for skin cancer diagnosis: first clinical evidence with spectroscopic data enhanced by machine learning algorithms

V. Mainardi[†,1,2], *Student Member, IEEE*, L. Carletti[†,1,2], *Student Member, IEEE*,
D. Tsiakmakis[1,2], *Student Member, IEEE*, M. Dal Canto[1], T. Melillo[1], S. Noferi[3], G. Bagnoni[4],
P. Rubegni[5] and G. Ciuti[1,2,6], *Senior Member, IEEE*

***Abstract*— Skin cancer represents a significant global health concern, with melanoma alone accounting for thousands of deaths annually. Early diagnosis is crucial for improving survival rates and reducing healthcare costs. While traditional diagnostic approaches involve visual inspection followed by biopsy, emerging technologies offer less invasive options with improved precision. In this study, a novel non-invasive device was designed, developed, and validated to employ near-infrared reflectance spectroscopy for skin lesion analysis. Furthermore, this work presents a machine learning approach aimed at classifying different types of skin lesions, as well as a new sequential approach to distinguish benign from malignant lesions based on spectral data and exploring the impact of anamnestic features. The device was used in two independent hospitals in Italy to collect data from 69 patients in total, including various types of skin lesions, all of whom followed the standard protocol for screening and diagnosis intervention. The implemented model achieved a recall of 93.8% and an accuracy of 75% for melanoma and benign classification, and a recall of 100% and an accuracy of 98.6% in distinguishing non-melanoma cancer from benign lesions, demonstrating promising results for skin cancer diagnosis utilizing spectral and anamnestic data. In summary, this study contributes to the development of allied non-invasive diagnostic tools and underscores the potential of machine learning in dermatology using spectroscopic data.**

I. INTRODUCTION

The global burden of cancer, based on GLOBOCAN 2020 data, reported about 1.5 million new cases of skin cancer in 2020, with 1.2 million non-melanoma skin cancers (excluding basal cell carcinoma) and >320k melanoma cases; melanoma alone accounted for >57k deaths during the same year [1]. The American Cancer Society (ACS) underscores the importance of early diagnosis to optimize survival rates and reduce healthcare costs: ACS reports a five-year survival rate >98.4% for localized melanoma [2], [3].

The standard diagnostic procedure for skin lesions involves qualitative visual inspection, followed by biopsy and histopathological assessment [4]. Dermoscopy, is a conventional tool to aid clinicians in skin lesion examination [5], [6], during which standardized diagnostic protocols, such as the 7-point checklist [7] or the ABCDE rule [6], are employed for identifying warning proxies of melanoma. Histological examination, despite its invasive nature and the time required for specimen interpretation, remains the gold standard for skin cancer diagnosis [4], [6]. Innovative technologies for skin cancer detection offer improved diagnostic precision. While the current visual assessment system combined with histological evaluation demonstrates a sensitivity of 84% [4], innovative technologies provide less invasive options and facilitate telemedicine [8]. These emerging techniques are classified based on physical or technological principles, including optical techniques (*e.g.*, VIS-NIR or Raman spectroscopy), skin electrical measurements techniques, thermal imaging, and photo-acoustic methods [8], [4], [5], [6]. Furthermore, computer-aided diagnosis in dermatology has been enhanced by automatic classification algorithms, providing an objective assessment during physicians' evaluations for early diagnosis of equivocal lesions. While various approaches have been proposed, most rely on images as input data, with only a few utilizing skin lesion spectra [6], [5]. Unlike optical imaging, spectroscopy can provide a more comprehensive analysis of lesion properties, such as composition, by detecting a broader range of the electromagnetic spectrum beyond the visible wavelength. In this article, the authors propose a novel non-invasive diagnostic device for the analysis of skin lesions utilizing NIR-reflectance spectroscopy; the device can also provide standard RGB-based imaging. In contrast, Raman spectroscopy yields weak and isolated signals due to its reliance on detecting Stokes and anti-Stokes scattering using highly efficient and sensitive instrumentation. McIntosh *et al.* [9] demonstrated that within the range of 400-1840 nm, six absorption bands display significantly different spectral responses between healthy and cancerous skin. Although significant progress has been achieved in developing image-based deep learning algorithms for skin tumour classification [6], [5], the lack of public databases containing spectral data for neural network pre-training prompted the authors to create an experimental measurement protocol in a clinical scenario. Machine learning (ML) techniques were employed to overcome the challenge posed by the limited availability of data. Consequently, the authors conducted a comprehensive investigation into the current State-of-the-Art (SoA) of reflectance spectroscopy techniques and automatic classification algorithms for skin cancer diagnosis (Table I). Numerous clinical classification tasks hold significant importance, primarily focusing on distinguishing between various types of skin cancers, including melanoma versus

[†]This authors contribute equally to the paper
[1] The BioRobotics Institute, Scuola Superiore Sant'Anna, 56025, Pisa, Italy (e-mail of corresponding authors: laura.carletti@santannapisa.it, vanessa.mainardi@santannapisa.it)
[2]Department of Excellence in Robotics & AI, Scuola Superiore Sant'Anna, 56025, Pisa, Italy
[3] Noze S.r.l., 56023, Pisa, Italy
[4]Dermatological Department of Spedali Riuniti, 57124, Leghorn, Italy
[5]Dermatological Department of Senese Hospital, 53100, Siena, Italy
[6]Health Science Interdisciplinary Center, Scuola Superiore Sant'Anna, 56127, Pisa, Italy

TABLE I

SOA SPECTRAL ANALYSIS OF SKIN CANCER, METHODS AND CLASSES

Authors	Dataset	Method and Classification algorithm	Classes
Boden *et. al.*, 2013 [10]	50	NIR and skin impedance spectroscopy: combined data Histopathology analyses of the lesions Multivariate technique: Principal Component Analysis (PCA) and Partial Least Square Discriminant Analysis (PLS-DA) using leave-one-out	Benign vs. Melanoma
Marchesini *et. al.*, 1992 [11]	62	Reflectance spectrophotometry 420-780nm, Global White Normalization Effective Spectrum for each lesion = Lesion reflectance data divided by the nearby healthy skin Histopathology analyses of only the suspicious lesions Stepwise discriminant analysis	Nevi vs. Melanoma
Carpenter *et. al.*, 2018 [12]	25	Diffusive Reflectance Spectroscopy, Global White Normalization Histopathology analysis of the lesions Non-linear least squares fit of the measured and modelled reflectance spectra to extract the absorber concentrations and the scattering parameters	Benign vs. BCC/SCC
Safi *et. al.*, 2016 [13]	3072	Diffuse Reflectance spectroscopy 178-1132 nm 3072 spectra (148 patients): 2926 normal moles and 146 malignant lesions 9/146 malignant lesions were histological proven melanoma, 137/146 were kept under observation PCA (2-5), SVM (linear, sigmoid, RBF and poly) cross-validation of 10 folds	Benign vs. Malignant
Shirkavand *et. al.*, 2017 [14]	40	Elastic scattering spectroscopy Singular Value Decomposition (SVD) and K-nearest neighbours (K-NN) analysis with 5 times repeat for clustering	Melanoma vs. Normal Skin

benign lesions, as well as non-melanoma skin tumours, such as basal cell carcinoma (BCC) and squamous cell carcinoma (SCC) versus benign lesions. Ultimately, the goal of establishing a generic classification to distinguish between benign and malignant lesions has secondary importance compared to discriminating between melanomas and non-melanoma tumours from benign lesions. Indeed, this discrimination remains the primary focus for accurate diagnosis and clinical management [8], as emphasized in the annual statistical reports by the World Health Organization (WHO) [1].

Within this framework, our research presents not only the development of a novel device for spectroscopic data acquisition but also classification techniques aimed at distinguishing melanomas from benign lesions (including nevi), as well as non-melanoma tumours (*i.e.*, BCC and SCC) from benign lesions, utilizing spectral data. Our methodology involves implementing SVM algorithms, customized to address each classification task individually, and drawing upon our initial database for training. Furthermore, our investigation delves into two distinct classification methodologies: a direct binary classification approach that discerns between malignant and benign lesions, and a sequential classification strategy. The latter employs previously developed algorithms to initially categorize lesions as either melanoma or benign, followed by a subsequent classification to differentiate between non-melanoma cancer versus benign lesions. This sequential methodology is designed to enhance diagnostic accuracy and overall classification performance. The article is structured as follows: Section II details the device for data acquisition, the web application for patient-related clinical data input, the experimental protocol, pre-processing steps, and ML algorithm selection. Section III and Section IV present the results and discussion. Concluding remarks and future directions are reported in Section V.

II. MATERIALS AND METHODS

This section offers a detailed outline of the architecture of the Data Collecting Tool (DCT), as depicted in Figure 1, along with the protocols used to collect and analyze data.

The data collection system comprises two main components: a hardware module, discussed in Section II-A, and a software module (*i.e.*, web app), described in Section II-B. Section II-C offers a comprehensive analysis of the experimental protocol employed for data collection. Finally, Section II-D presents the ML models implemented for skin lesion classification.

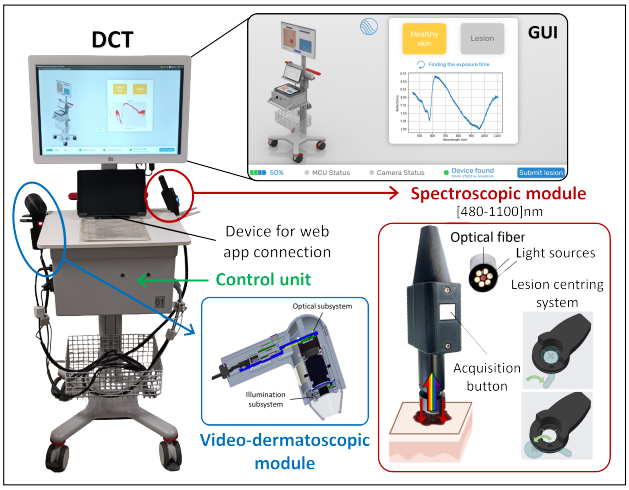

Fig. 1. Data Collecting Tool (DCT): video-dermatoscopic module, spectroscopic module, control unit, GUI and lesion centring system.

A. Data collecting system

The device was certified for compliance with IEC 62133-2:2017, UL 62133, and IEC 60601-1 standards. Battery management was conducted in accordance with the System Management Bus (SMBus) protocol. The medical trolley is compliant with the IEC 60601-1 standard and with the 93/42/CE medical device directive. The DCT embeds three modules: *i)* the main unit with the Graphical User Interface (GUI); *ii)* the videodermatoscopic module; and *iii)* the spectroscopic module, source of the analysed data in this study.

The main unit is a general-purpose hardware that incorporates a computing platform (Jetson Nano, NVIDIA,

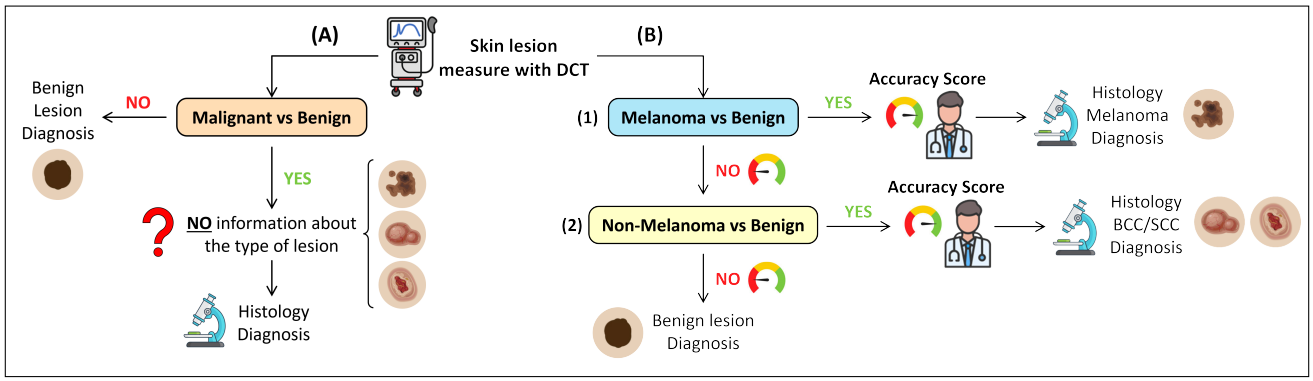

Fig. 2. Different classification approach of skin lesions: (A) binary method (*i.e.*, malignant vs. benign), (B) sequential method (*i.e.*, melanoma vs. benign and non-melanoma vs. benign)

California, U.S.A), a Wi-Fi radio, a power management system, GPIO ports, 12 VDC fans, and USB 2.0 and USB 3.0 cables for powering, management, image transmission, and streaming of the videodermatoscopic and spectroscopic modules. Two batteries (PH3059QE26, Inspired Energy, Florida, U.S.A.) were connected via a 7W2D-sub mixed contacts connector to two smart charger PCBs (EB292A4.4, Accutronics, Staffordshire, U.K.), which constituted the power management system. The battery output voltage (28.8 VDC) was divided into various voltages (12 VDC, and 5 VDC) using 2 DC-DC converters (TracoPower Ltd, Baar, Switzerland): the 12 VDC line powers the touchscreen, the spectroscopy light source, and fans, and the 5 VDC line powers the 7-port industrial USB 3.0 Hub and the computing platform. An onboard temperature sensor monitored temperatures inside the enclosure and regulated the fan speed through the internal microcontroller based on device heating. Furthermore, the main unit includes an external display for real-time observation of the RGB stream from the camera and the spectrum through a user-friendly GUI designed in collaboration with medical doctors, and houses a tablet with the web app. The GUI was written in Python language and acquired data was stored in a local folder until a network connection was available. Once the connection was stable, data were promptly transferred to the web app back-end and deleted from the local folder to preserve memory space and enhance privacy protection.

The videodermatoscopic module comprises an optical subsystem and an illumination subsystem. The optical subsystem includes a RGB camera (Jazz, Alkeria s.r.l., Pisa, Italy), integrated with a CMOS camera sensor (SONY IMX264LLR/LQR, Phase 1 Technology Corporation, New York, U.S.A.), and a Basler lens (Basler AG, Ahrensburg, Germania), compatible with the CMOS sensor. This setup is designed to provide a field of view similar to that of standard dermatoscopes (15 mm x 15 mm). Additionally, polarizing filters and light diffusers are integrated and a spacer is used to maintain a fixed distance between the imaging sensor and the skin. The illumination subsystem consists of a PCB illuminator housing an array of 18 white LEDs, two drivers (LP55231SQX, Texas Instruments, Texas, U.S.A) for controlling the luminous emission intensity of the LEDs. These drivers are managed via the I2C protocol using pulse-width modulation (PWM) from a microcontroller (ATSAMD21G18, Microchip Technology, Arizona, U.S.A.). The entire system is encased within a 3D printed enclosure, crafted using stereolithography technology (Form 3+, Formlabs, Massachusetts, U.S.A.) to ensure ergonomic handling by clinicians.

For the spectroscopic module, near-infrared spectroscopy was selected as preferred technique. Consequently, the Qmini device (Qmini AFBR-S20M2VN, Broadcom, California, U.S.A.), working in the 480-1100 nm range, was chosen as the most suitable for the purposes of this study. This spectroscope required an external light source and a bifurcated optical fiber for operation. The light source (HL 2000-LL halogen bulb, Ocean Insight, Florida, U.S.A) covers the range from 360 to 2400 nm and boasts a 10,000-hour lifetime. It is equipped with a frontal SMA-905 optical fiber connector (Thorlabs, New Jersey, U.S.A) designed to accommodate multimode optical fiber bundles. The bifurcated optical fiber consists of a reflection probe housing receiving and transmitting fibers, along with two split ends featuring an SMA-905 connector: one end connects to the light source, while the other connects to the spectroscope. A VIS/NIR reflection probe with a 400 µm core diameter and a length of 2 meters was used. The probe was integrated into a 3D printed handle (FDM technology, Zortrax M200+ printer, Olsztyn, Poland) and tested by clinicians to enhance ergonomics and usability. The skin and lesion spectra were normalized using the optical blank acquired at the hospitals during installation.

B. Web app

The web app was designed to facilitate the patient data acquisition process during clinical trials. The front-end served as a guide for clinicians throughout the data acquisition procedure and interacted with the back-end infrastructure for data storage. To ensure responsive and engaging user interfaces, the web app was built on top of REST/GraphQL APIs using JavaScript ES6 and web components. These web components are a collection of web platform APIs that enable the creation of custom, reusable, encapsulated HTML tags for use in web pages and apps. React/Redux, an open-source project, was utilized for this purpose. The web app's design adhered to the UX design framework Material and Material-UI, an open-source system of guidelines, components, and

tools that promote best practices in user interface design. Moreover, the web app was developed as a safe progressive web application, functional both online and offline, accessible via tablets, computers, and smartphones.

C. Experimental protocol

The experimental protocol comprises several phases for acquiring and evaluating data: skin lesions of participating patients. Initially, informed consent is obtained through paper documentation. The front-end on the web app, accessible via a tablet with a doctor account, facilitates various tasks: *i)* gathering the patient's medical history; *ii)* delineating the body area under investigation, segmented into 17 zones via an interactive rendering of the human figure; and *iii)* capturing macroscopic images of the lesions along with relevant anamnestic data. Dermatoscopic images of the lesions are captured using the videodermatoscopic module of the device, whereas spectra of both the lesion and the surrounding healthy skin are collected utilizing the spectroscopic module as part of the same device. A 3D-printed centring add-on, shown in Figure 1, was designed to ensure a perfect alignment of the spectroscopic probe with the lesion, enabling precise and stable spectrum acquisition. After the data acquisition, a QR code, generated by the GUI, enables the unique association of the collected data with the patient profile created via the web app. Ultimately, the diagnosis of the lesions is established through biopsy, as in standard practice, and retrospectively linked to the patient using the front-end on the web app.

D. Data analysis

This study was approved by the Regional Ethical Committee for Clinical Experimentation in Tuscany (protocol: iDCNN dermoscopy, number: 18534, 18/01/2021) and, consequently applied both in the Departments of Dermatology in Siena and also in the Departments of Dermatology in Leghorn (in this case, prior adaptation of the information sheet, informed consent and privacy policy by the hospital privacy manager). The data were anonymized to protect patient privacy. The spectrum of the lesions, the anamnestic data of the patient and the lesion, and a combination of the previous two datasets were analysed to automatically classify: *i)* melanoma and benign lesions; *ii)* melanoma and nevi; *iii)* non-melanoma skin cancers (BCC and SCC) and benign lesions; and *iv)* malignant and benign lesions. Two distinct approaches for classification were implemented simultaneously: *i)* a sequential approach, which distinguishes malignant lesions into melanoma and non-melanoma before comparing them to benign lesions; and *ii)* a binary method that directly discriminates between malignant and benign lesions (Figure 2). The classification order was defined to prioritise accurate and early identification of melanoma, due to its distinctive importance in patients' healthcare for timely intervention; however, the order does not affect the algorithm outcomes. A representative feature learning approach based on kernel PCA was conducted using the spectrum of the lesions for noise reduction and to extract the most relevant features. Due to the unbalanced nature of the dataset for the different classification goals, multiple oversampling techniques were applied, such as the duplication or triplication of the minority class, filtering the spectrum using Savitzky–Golay filter with a window length of 40 and polyorder equal to 2. During the training phase, a leave-one-out cross-validation strategy was implemented with SVM, and the tuning of the hyper-parameters was carried out considering three kernels (*i.e.*), linear, radial basis function, and polynomial) with degrees ranging from 1 to 4. The regularization parameters C (*i.e.)*, trade-off between achieving a good fit to the training data and a simple decision boundary) and gamma (*i.e.)*, width of the kernel function) were varied within ranges of [0.001, 0.01, 0.1, 1, 10] and [0.1, 0.2, 0.3, 0.4, 0.5], respectively. The performance of the algorithms on the test set was assessed using standard metrics, such as accuracy (*i.e.*, the ratio of true predictions to all predictions) and recall (*i.e.*., the ratio of true positives to the sum of true positives and false negatives). The workflow is depicted in Figure 3. The analyses were performed on a server Intel(R) Xenon(R) gold 5217 equipped with a 3.00 GHz CPU and 128 GB of memory.

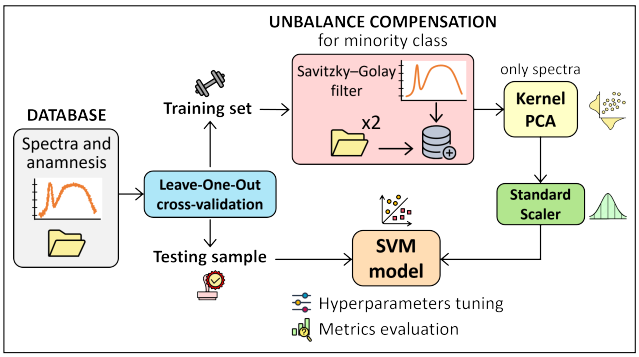

Fig. 3. Workflow for classification algorithms. The database is divided in training and test sets. The training set is balanced and relevant features are extracted with PCA.

III. RESULTS

Data were collected at the Spedali Riuniti of Leghorn (Leghorn, Italy) and the Senese Hospital in Siena (Siena, Italy) from October 2022 to January 2023. Lesions from 69 patients (average age of 56.9 years, with 70% of them male), already screened and selected to undergo biopsy, were included in the study with DCT. Specifically, spectra of the lesions and of the surrounding healthy skin were acquired. Complete medical history data were also collected and documented for all patients, including age, sex, skin phototype (1-4), skin type, body mass index (BMI), hair and eye colour, as well as risk factors such as personal and family history of melanoma, exposure to sunlight during childhood, consumption of red wine, and smoking habits. Within the collected database of 69 lesions, comparable in size to the SoA, the following were identified: 28 nevi (NEV); 11 Basal Cell Carcinomas (BCC); 2 Squamous Cell Carcinomas (SCC); 16 Malignant Melanomas (MEL); 5 Seborrheic Keratoses (BKL); 1 Actinic Keratosis (AK); 3 vascular lesions (VASC); and 3 cases of unknown origin (UNK), not imputable to the previous categories. The malignant lesions include MEL, BCC, and SCC (29 in total),

TABLE II

SUMMARY OF THE PERFORMANCES FOR EACH CLASSIFICATION TASK, DATASET AND ALGORITHM

Classification task	Lesions	Dataset	Algorithm	Accuracy	Recall
Malignant vs. Benign	69	anamnesis	SVM: C=1, kernel=poly, degree=2 , gamma=0.3	62.3%	79.3%
		spectrum	10 PCs, SVM: C=0.017, kernel=poly, degree= 2, gamma=0.2	71%	86.2%
		spectrum and anamnesis	5 PCs, SVM: C: 0.1, kernel: linear, gamma: 0.1, degree: 2	66.7%	93.1%
Melanoma vs. Nevi	44	anamnesis	SVM: C=0.001, kernel=poly, degree=4 , gamma=0.4	93.2%	81.3%
		spectrum	18 PCs, SVM: C=1, kernel=rbf, degree= 2, gamma=0.3	86.4%	81.3%
		spectrum and anamnesis	3 PCs, SVM: C=1, kernel=poly, degree=3 , gamma=0.3	75%	100%
Melanoma vs. Benign	56	anamnesis	SVM: C=0.0005, kernel=poly, degree=4 , gamma=0.54	89.3%	87.5%
		spectrum	15 PCs, SVM: C=0.01, kernel=poly, degree=2, gamma=0.5	69.6%	87.5%
		spectrum and anamnesis	3PCs, SVM: C=1, kernel=poly, degree= 3, gamma=0.3	75%	93.8%
BCC/SCC vs. Benign	53	anamnesis	SVM: C=0.001, kernel=poly, degree=4, gamma=0.5	67.9%	84.6%
		spectrum	4PCs, SVM: C=0.001, kernel=poly, degree=3, gamma=0.1	96.2%	100%
		spectrum and anamnesis	4PCs, SVM: C=0.001, kernel=poly, degree=3, gamma=0.1	98.1%	100%

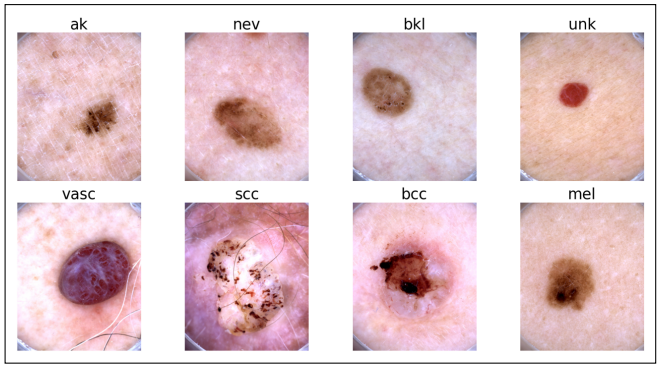

Fig. 4. Different types of skin lesions collected with the DCT

while the remainder were classified as benign lesions (40 in total). All the collected data types are shown in Figure 4.

For each classification task, we employed 3 initial databases and varied balancing techniques. Initially, we examined the impact of spectra obtained through our device. Then, we assessed the performance of the most relevant clinical anamnestic features, including prior personal or familial history of melanoma, sex, childhood sunburns, smoking, and rapid growth of the lesion. Finally, we evaluated the synergistic effect of combining these two types of information to establish the efficacy of spectral data in diagnosis.

In the context of binary classification, for distinguishing between benign skin lesions and melanoma, the anamnestic dataset provided accuracy and recall of 89.3% and 87.5%, respectively, through duplicating the malignant lesion dataset. Spectra yielded accuracy and recall of 69.6% and 87.5%, respectively, under similar conditions. Meanwhile, combining anamnesis and spectra, the authors achieved an accuracy of 75% and a recall of 93.8% with a tripled malignant lesion dataset. When distinguishing nevi from melanoma, anamnestic data achieved 93.2% accuracy and 81.3% recall. Spectra yielded 86.4% accuracy and 81.3% recall by doubling the malignant lesion dataset. The combination of anamnesis and spectra achieved 75% accuracy and 100% recall with a tripled malignant lesion dataset. In discriminating non-melanoma skin lesions from benign lesions, anamnestic data achieved 67.9% accuracy and 84.6% recall by tripling the malignant lesion dataset. Spectra reached 96.2% accuracy and 100% recall under the same conditions. Lastly, the combination of anamnesis and spectra achieved 98.1% accuracy and 100% recall by doubling the malignant lesion dataset. Within the framework of binary classification, for distinguishing between benign and malignant skin lesions, anamnestic data reached 62.3% accuracy and 79.3% recall. Spectra achieved 71% accuracy and 86.2% recall. The combination of anamnesis and spectra reached 66.7% accuracy and 93.1% recall by tripling the malignant lesion dataset. All the performance and the parameters of the model are summarized in Table II.

IV. DISCUSSION

Results underscored promising benefit in using spectroscopy for accurately distinguishing various types of skin tumours. Following a systematic approach, multiple algorithms were developed with varying performances depending on the specific task. Integrating anamnestic data into the spectroscopy database improved recall performance, although it slightly decreased classification accuracy; this effect is particularly notable in melanoma classification, likely due to the influence of genetics and family history on melanoma risk. Given the application's need to correctly identify potentially malignant lesions, prioritizing recall over accuracy was deemed essential. The confusion matrices corresponding to the 4 classification tasks, derived from the combination of spectral and anamnestic data, are depicted in Figure 5, whereas the performances are compared with the SoA in Table III. Notably, the authors successfully discriminated non-melanoma skin cancers (BCC/SCC) from benign lesions, and melanomas from common nevi and benign lesions with performances overcoming the relative SoA. Due to the close resemblance between melanoma and benign nevi, the performance in binary classification between malignant and benign lesions was slightly lower compared to state-of-the-art methods. It is worth mentioning that the authors' primary goal was to identify nearly all malignant lesions accurately, prioritizing the recall parameter over improving overall classification performance through accu-

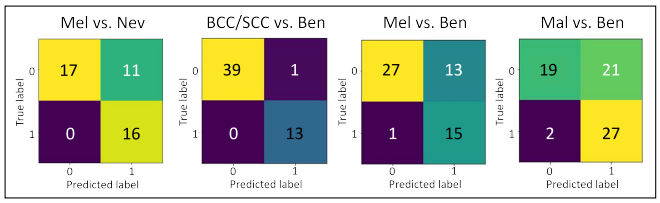

Fig. 5. Confusion Matrix for the classification tasks with the combination of anamnesis and spectra as dataset

racy enhancements. This outcome was expected, considering the diverse characteristics, including visual ones, exhibited by malignant lesions, particularly between melanomas and BCC/SCC, as corroborated by WHO global statistics on skin cancer, which categorize these entities separately. In summary, these results demonstrated the effectiveness of a sequential double classification approach compared to a single binary method (*i.e.*, benign vs. malignant), without increasing computational complexity.

TABLE III

COMPARISON BETWEEN OUR PERFORMANCE AND SOA

Main principles	SoA Performance	Our Performance
Only 9 lesions were histological analysed [13]	Accuracy: 94.9%	Accuracy: 66.7% Recall: 93.1%
Limited to linear relationship between variable and risk of overfitting [11]	Sensitivity: 90.3% Specificity: 77.4%	Recall: 100% Accuracy: 75%
Unbalanced dataset and limited to linear relationship [10]	Sensitivity: 83% Specificity: 95%	Recall: 93.8% Accuracy: 75%
Limited to specific function form and assumption and risk of overfitting [12]	Sensitivity: 92% Specificity: 54%	Recall: 100% Accuracy: 98.1%

V. CONCLUSIONS

This study contributes to the ongoing development of non-invasive spectroscopy-based diagnostic tools in dermatology and underscores the potential of machine learning techniques in improving skin cancer diagnosis by combining spectral (obtained by an innovative dermatoscopic device, *DCT*) and anamnestic data. Furthermore, this work highlights the effectiveness of a sequential double classification approach over binary methods, particularly in distinguishing melanomas and non-melanoma skin cancers (BCC/SCC) from benign lesions due to the diverse characteristics exhibited by malignant lesions. Feasibility of an innovative diagnostic approach has been demonstrated, and the developed DCT device has initiated the groundwork for creating a spectral database to support future implementation of AI algorithms. Future research will focus on expanding the dataset and exploring additional techniques, such as Representative Feature Learning and Deep Learning, for classification. Integrating multi-source data may contribute to facilitate faster and more accurate clinical assessments, reducing diagnostic times and improving patient clinical outcomes.

FUNDING

This work was carried on in the framework of the Advanced Laboratory Automation project funded by INPECO SA (Novazzano, Switzerland).

ACKNOWLEDGMENT

The authors would like to thank INPECO SA (Novazzano, Switzerland - www.inpeco.com) as the formal promoter of a strategic industrial initiative on P5 medicine applied to dermatology. In addition, the authors acknowledge the support of the BRIEF "Biorobotics Research and Innovation Engineering Facilities" project (Project identification code: IR0000036) funded under the National Recovery and Resilience Plan (NRRP), Mission 4 Component 2 Investment 3.1 of Italian Ministry of University and Research funded by the European Union - NextGenerationEU.

REFERENCES

[1] H. Sung, J. Ferlay, R. L. Siegel, M. Laversanne, I. Soerjomataram, A. Jemal, and F. Bray, "Global cancer statistics 2020: Globocan estimates of incidence and mortality worldwide for 36 cancers in 185 countries," *Cancer Journal for Clinicians*, vol. 71, pp. 209–249, 2021.

[2] American Cancer Society, "Survival rates for melanoma skin cancer." [Online]. Available: https://www.cancer.org/cancer/types/melanoma-skin-cancer/detection-diagnosis-staging/survival-rates-for-melanoma-skin-cancer-by-stage.html

[3] Melanoma Research Alliance, "Melanoma survival rates," 2024. [Online]. Available: https://www.curemelanoma.org/about-melanoma/melanoma-staging/melanoma-survival-rates

[4] D. N. Dorrell and L. C. Strowd, "Skin cancer detection technology," *Dermatologic Clinics*, vol. 37, pp. 527–536, 2019.

[5] V. Narayanamurthy, P. Padmapriya, A. Noorasafrin, B. Pooja, K. Hema, A. Y. F. Khan, K. Nithyakalyani, and F. Samsuri, "Skin cancer detection using non-invasive techniques," *RSC Advances*, vol. 8, pp. 28 095–28 130, 2018.

[6] L. Rey-Barroso, S. Peña-Gutiérrez, C. Yáñez, F. J. Burgos-Fernández, M. Vilaseca, and S. Royo, "Optical technologies for the improvement of skin cancer diagnosis: A review," *Sensors*, vol. 21, p. 252, 2021.

[7] G. Argenziano, G. Fabbrocini, P. Carli, V. D. Giorgi, E. Sammarco, and M. Delfino, "Epiluminescence microscopy for the diagnosis of doubtful melanocytic skin lesions: Comparison of the abcd rule of dermatoscopy and a new 7-point checklist based on pattern analysis," *Archives of Dermatology*, vol. 134, pp. 1563–1570, 1998.

[8] A. Blundo, A. Cignoni, T. Banfi, and G. Ciuti, "Comparative analysis of diagnostic techniques for melanoma detection: A systematic review of diagnostic test accuracy studies and meta-analysis," *Frontiers in Medicine*, vol. 8, p. 637069, 2021.

[9] L. M. McIntosh, R. Summers, M. Jackson, H. H. Mantsch, J. R. Mansfield, M. Howlett, A. N. Crowson, and J. W. Toole, "Towards non-invasive screening of skin lesions by near-infrared spectroscopy," *The Journal of investigative dermatology*, vol. 116, pp. 175–181, 2001.

[10] I. Bodén, J. Nyström, B. Lundskog, V. Zazo, P. Geladi, B. Lindholm-Sethson, and P. Naredi, "Non-invasive identification of melanoma with near-infrared and skin impedance spectroscopy," *Skin Research and Technology*, vol. 19, pp. e473–e478, 2013.

[11] R. Marchesini, N. Cascinelli, M. Brambilla, C. Clemente, L. Mascheroni, E. Pignoli, A. Testori, and D. R. Venturoli, "In vivo spectrophotometric evaluation of neoplastic and non-neoplastic skin pigmented lesions. ii: discriminant analysis between nevus and melanoma," *Photochemistry and Photobiology*, vol. 55, pp. 515–522, 1992.

[12] D. J. Carpenter, M. B. Sajisevi, N. Chapurin, C. S. Brown, T. Cheng, G. M. Palmer, D. S. Stevenson, C. L. Rao, R. P. Hall, and C. R. Woodard, "Non-invasive optical spectroscopy for identification of non-melanoma skin cancer: Pilot study," *Lasers in Surgery and Medicine*, vol. 50, pp. 246–252, 2018.

[13] A. Safi, S. Ziauddin, A. Horsch, M. Ziai, V. Castaneda, T. Lasser, and N. Navab, "Feasibility study of optical spectroscopy as a medical tool for diagnosis of skin lesions," *International Journal of Advanced Computer Science and Applications*, vol. 7, 2016.

[14] A. Shirkavand, S. Sarkar, L. Ataie-Fashtami, and H. Mohammadreza, "Detection of melanoma skin cancer by elastic scattering spectra: A proposed classification method," *Iranian Journal of Medical Physics*, vol. 14, pp. 162–166, 2017.